

Determination of stress in thin films using micro-machined buckled membranes

Citation for published version (APA):

Malhaire, C., Granata, M., Hofman, D., Amato, A., Martinez, V., Cagnoli, G., Lemaitre, A., & Shcheblanov, N. (2023). Determination of stress in thin films using micro-machined buckled membranes. *Journal of Vacuum Science & Technology A*, 41(4), Article 043401. <https://doi.org/10.1116/6.0002590>

Document status and date:

Published: 01/07/2023

DOI:

[10.1116/6.0002590](https://doi.org/10.1116/6.0002590)

Document Version:

Publisher's PDF, also known as Version of record

Document license:

Taverne

Please check the document version of this publication:

- A submitted manuscript is the version of the article upon submission and before peer-review. There can be important differences between the submitted version and the official published version of record. People interested in the research are advised to contact the author for the final version of the publication, or visit the DOI to the publisher's website.
- The final author version and the galley proof are versions of the publication after peer review.
- The final published version features the final layout of the paper including the volume, issue and page numbers.

[Link to publication](#)

General rights

Copyright and moral rights for the publications made accessible in the public portal are retained by the authors and/or other copyright owners and it is a condition of accessing publications that users recognise and abide by the legal requirements associated with these rights.

- Users may download and print one copy of any publication from the public portal for the purpose of private study or research.
- You may not further distribute the material or use it for any profit-making activity or commercial gain
- You may freely distribute the URL identifying the publication in the public portal.

If the publication is distributed under the terms of Article 25fa of the Dutch Copyright Act, indicated by the "Taverne" license above, please follow below link for the End User Agreement:

www.umlib.nl/taverne-license

Take down policy

If you believe that this document breaches copyright please contact us at:










repository@maastrichtuniversity.nl

providing details and we will investigate your claim.



RESEARCH ARTICLE | MAY 19 2023

Determination of stress in thin films using micro-machined buckled membranes

C. Malhaire   ; M. Granata  ; D. Hofman  ; A. Amato  ; V. Martinez  ; G. Cagnoli  ; A. Lemaitre  ;
N. Shcheblanov 



J. Vac. Sci. Technol. A 41, 043401 (2023)

<https://doi.org/10.1116/6.0002590>



View
Online



Export
Citation

CrossMark







Determination of stress in thin films using micro-machined buckled membranes

Cite as: J. Vac. Sci. Technol. A 41, 043401 (2023); doi: 10.1116/6.0002590

Submitted: 15 February 2023 · Accepted: 18 April 2023 ·

Published Online: 19 May 2023



C. Malhaire,^{1,a)}  M. Granata,²  D. Hofman,²  A. Amato,^{3,b)}  V. Martinez,³  G. Cagnoli,³  A. Lemaitre,⁴ 
and N. Shcheblanov^{4,5} 

AFFILIATIONS

¹Univ Lyon, INSA Lyon, CNRS, Ecole Centrale de Lyon, Université Claude Bernard Lyon 1, CPE Lyon, INL, UMR5270, 69621 Villeurbanne, France

²Laboratoire des Matériaux Avancés-IP2I, CNRS, Université de Lyon, Université Claude Bernard Lyon 1, F-69622 Villeurbanne, France

³Université de Lyon, Université Claude Bernard Lyon 1, CNRS, Institut Lumière Matière, F-69622 Villeurbanne, France

⁴Navier, Ecole des Ponts, Université Gustave Eiffel, CNRS, Marne-la-Vallée, France

⁵MSME, UMR 8208, Université Gustave Eiffel, CNRS, Université Paris-Est Créteil, Marne-la-Vallée, France

^{a)}Author to whom correspondence should be addressed: christophe.malhaire@insa-lyon.fr

^{b)}Current affiliation: Maastricht University, P.O. Box 616, 6200 MD Maastricht, The Netherlands.

ABSTRACT

In this work, optical profilometry and finite-element simulations are applied on buckled micromachined membranes for the stress analysis of ion-beam-sputtered Ta₂O₅ and SiO₂ thin films. Layers with different thicknesses are grown on silicon substrates, and then several membranes with different geometries are manufactured with standard microsystem technologies; due to a high level of films' compressive stress, buckled membranes are obtained. Thermally grown silica membranes are also produced for comparison. The residual stress values are determined by comparing the measured and simulated deflections of the membranes. The average stress state of Ta₂O₅ thin films is found to be −209 MPa. The SiO₂ thin films are in a higher compressive stress state whose average value is −576 MPa. For comparison, the average stress in thermal SiO₂ thin layers grown at 1130°C is found equal to −321 MPa, in good agreement with the literature.

Published under an exclusive license by the AVS. <https://doi.org/10.1116/6.0002590>

I. INTRODUCTION

The current high-reflection (HR) coatings of the Advanced LIGO, Advanced Virgo, and KAGRA gravitational-wave detectors^{1–3} are thickness-optimized Bragg reflectors⁴ of alternating layers of ion-beam-sputtered (IBS) tantalum pentoxide (Ta₂O₅, also known as *tantala*, with high refractive index n_H) and silicon dioxide (SiO₂, *silica*, low refractive index n_L), grown by the Laboratoire des Matériaux Avancés⁵ (LMA).^{6,7} Despite their excellent optical and mechanical properties,^{7–9} their Brownian thermal noise¹⁰ constitutes a severe limitation to the sensitivity of current and future gravitational-wave detectors. Thus, in the last two decades, a considerable research effort has been committed to select and develop alternative coating materials featuring even lower mechanical and optical losses at the same time.^{11,12} The need to develop alternative coating materials is even stronger for cryogenic gravitational-wave detectors,

either present or future, such as KAGRA,³ Einstein Telescope,^{13,14} and Cosmic Explorer.¹⁵ The accurate estimation of residual stress in thin films falls within this context.

In the past, many studies were conducted to determine the stress of tantala and silica coatings. For both materials, the stress is generally compressive (here, negative by convention).

Concerning tantala, a stress value of −250 MPa was reported by Ngaruiya *et al.* for 100 nm thick films grown via reactive DC magnetron sputtering;¹⁶ more precisely, they observed that the stress decreases with an increasing oxygen flow rate and becomes almost constant at −250 MPa for an oxygen flow greater than 6 SCCM. For a 4800 nm thick film grown via RF magnetron sputtering, Cheng *et al.* measured stress values ranging from −314 MPa at 25°C to −346 MPa at 100°C.¹⁷ In a work by Farhan *et al.* on 200–350 nm thick films grown by ion beam-assisted deposition, it

22 February 2024 08:39:37

was found that stresses increase with ion current density from -280 to -375 MPa.¹⁸

Concerning silica, films with low stress (ranging from -490 to -48 MPa) and high optical quality were obtained by IBS using high-energy O₂ ion bombardment during deposition.¹⁹

In 2005, the stress level of IBS silica and tantalum thin layers in the HR coatings of the LIGO interferometer was determined by Netterfield *et al.* before and after a postdeposition thermal treatment (*annealing* hereafter) was applied.²⁰ They showed that a tantalum film can readily go from a compressive state to a tensile state after only moderate annealing, whereas the compressive silica films stress is slightly relaxed and remains compressive. It was also pointed out that for multilayer HR coatings composed of several silica/tantalum doublets, the net postanneal stress depends on the silica to tantalum thickness ratio.

Netterfield *et al.* also argued that different annealing regimes adopted by various coating suppliers might lead to quite large variations in residual stress, thus explaining the differences in mechanical loss observed for similar multilayer coatings. More recently, Granata *et al.* showed that measured coating dissipation in HR multilayer coatings is usually higher than expectation,^{9,21} and that their stress level could be loosely correlated with the measured excess loss.²¹

Finally, it is known that residual stresses can promote the appearance of cracks during annealing.^{22–24}

In all the works cited above, the substrate curvature method associated with Stoney's formula was employed to quantify the stress state of the films. Indeed, this is a well-known, nondestructive method used to determine the stress level of a thin film on a thick substrate, sometimes even in the case where the hypotheses of the model are not completely satisfied.²⁵ However, apart from assumptions of the model, this method suffers from a few practical flaws: dependence on the substrate parameters (thickness nonuniformity is critical, as it is squared in Stoney's equation) and repeatability of measurements (a three-point support is essential). Therefore, it is generally more useful for differential measurements (before and after annealing, for instance) than for absolute stress measurements.

In this paper, we present an alternative method for the determination of compressive stresses in thin films. It consists of manufacturing buckled membranes by locally etching the substrate under thin films and of comparing the measured deflection profiles of the membranes with those obtained by finite element simulations. Note that for films with a residual tensile stress, flat membranes would be obtained, and other characterization methods could be used: vibrometry,²⁶ bulge-test,²⁷ or point-deflection²⁸ methods, for example.

II. EXPERIMENT

A. Samples

After a standard cleaning procedure, 50 mm, double-side polished, silicon wafers were thermally oxidized on both sides ($1.5\ \mu\text{m}$ thick films grown at 1130°C in wet atmosphere). The backside SiO₂ layer was patterned to open square windows of various dimensions. On the front side, the oxide layer was either left pristine, in order to study the stress state of the thermal SiO₂ for comparison, or completely removed before deposition of IBS Ta₂O₅ or SiO₂ layers.

The IBS Ta₂O₅ and SiO₂ thin films studied in this work were grown by the LMA, in a commercial Veeco SPECTOR system, using accelerated, neutralized argon ions as sputtering particles. Prior to deposition, the base pressure inside the vacuum chamber was lower than 10^{-5} mbar. Argon was fed into the ion-beam source while oxygen was fed into the vacuum chamber for a total residual working pressure of the order of 10^{-4} mbar. The energy and current of the sputtering ions were 1.3 keV and 0.6 A, respectively.

In a following step, the substrate was etched from the back side, through the oxide mask, using an aqueous potassium hydroxide solution (KOH, 34 wt. % at 60°C) until self-supporting membranes were obtained out of thin films. During the hour-long etch process, the front side of the wafer was protected from KOH by means of a sample holder. More precisely, to prevent the rupture of a membrane from compromising the entire substrate, the production of membranes was generally performed in two stages: a first long etching step, leaving only a few tens of micrometers of silicon, after which the substrate was cut, so as to complete the separation of each chip individually. A schematic view and a photo of a single-chip sample holder is shown in Fig. 1 (a bigger sample holder was used for the 2" substrate).

After a few tests, the membrane dimensions (side, thickness) were determined so as to guarantee that the compressive stress in the material caused moderate buckling,²⁹ thereby avoiding their rupture during the fabrication process, and obtain reproducible deformed profiles. Indeed, for very thin membranes, the slightest imperfection in their geometry [due to a misalignment of the photolithography mask parallel to the (110) direction, inhomogeneous over-etching, thickness inhomogeneities, etc.] might lead to a profile that is not symmetrical enough to be correctly measured and simulated. That was the case for two 250 nm thick, $140\ \mu\text{m}$ side length, SiO₂ membranes, for instance, which were so strongly and randomly deformed that they could not be used in this study. So, as a general rule, the more stressed and thinner the film, the less the chance of obtaining membranes with an usable profile. Here, we present results from membranes with thicknesses ranging from about 1 to $2\ \mu\text{m}$. After dicing, the 3D profile of each membrane was measured by means of a Wyko NT-1100 white-light profilometer (that is, an interferometric microscope). For this device, the in-plane resolution depends on magnification. Typically, $10\times$ magnification was used, corresponding to a $0.84 \times 0.98\ \mu\text{m}^2$ resolution. For the few smaller membranes, $25\times$ magnification was used with a resolution of $0.34\ \mu\text{m} \times 0.39\ \mu\text{m}$. The vertical resolution is independent of the used objectives and is nanometric. Due to the measurement noise, but especially to the calibration procedure of the device (using a step height standard), the relative uncertainty on the deflection of the membrane is estimated at 0.25%.

Samples' characteristics are summarized in Table I. The measured deflection refers to maximum deflection measured at the center of the samples. Note that Table I only lists a few typical samples with mostly distinct geometries, whereas several other similar samples were produced. The results are very reproducible: for example, five SiO₂-S21056 membranes (not shown) having the same side size within a 0.75% uncertainty featured same stress-induced deflection within a 1.0% uncertainty. Likewise, the profiles of samples Ta₂O₅-S20061-6 and -15 as well as samples Ta₂O₅-S20061-7 and -9 are very similar.

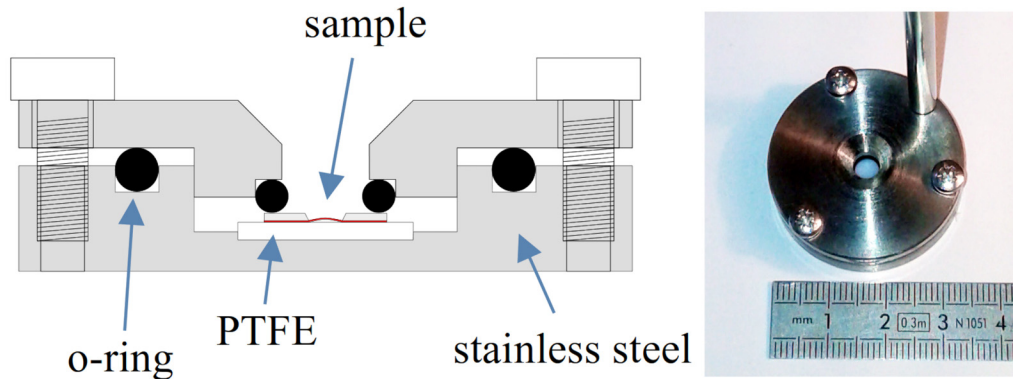


FIG. 1. Schematic view and photo of a single-chip sample holder.

B. Methods

The refractive index and thickness of IBS thin films were measured via transmission spectrophotometry through samples grown on fused-silica witness samples. Using Perkin Elmer Lambda 1050 spectrophotometer, the spectra were acquired at normal incidence in the 400–1400 nm wavelength range. The refractive index and thickness were first evaluated using the envelope method,³⁰ and then those results were used as initial values in a numerical least-square regression analysis. In the model, the adjustable parameters were the film thickness and the (B_i , C_i) coefficients of the Sellmeier dispersion equation,

$$n^2 = 1 + \sum_{i=1}^3 \frac{B_i \lambda^2}{\lambda^2 - C_i}, \quad (1)$$

where n is the thin film refractive index and λ is the wavelength.

Finite-element simulations were performed using ANSYS 2022R1 software. The meshing of the micromachined membrane was carried out either with 2D (SHELL281) or 3D (SOLID186) elements. In both cases, for a given stress value, the simulated profiles were similar. As the thickness/width ratio of the membranes was small, shell elements were the most effective choice in terms of computation time. The silicon surrounding the membrane was meshed with the 3D elements. In a first static analysis, a very low pressure was applied to the unstressed membrane, in order to obtain a very small downward predeflection; then, the geometry of the model was updated. By initially introducing a slight imperfection in the model, it is possible to subsequently obtain a downward buckling of the membrane, as observed experimentally. The membranes were systematically oriented downward due to the presence of the sample holder during etching (Fig. 1). Since the sample is sandwiched and clamped against a support, deformation of the membrane can only occur in one direction. Finally, a nonlinear

22 February 2024 08:39:37

TABLE I. Measured (thickness, size, and deflection) and estimated (stress) properties of self-supporting thin membranes.

Material	Sample ID	Thickness (nm)	Side length (μm)	Measured deflection (μm)	Stress (MPa)	
IBS Ta ₂ O ₅	S20061-07	1008	390.1 ± 2.0	-9.5 ± 0.1	-206	
	S20061-09	1008	395.4 ± 2.0	-9.5 ± 0.1	-206	
	S20061-14	1008	297.0 ± 2.0	-7.3 ± 0.1	-208	
	S20061-06	1008	193.5 ± 2.0	-4.7 ± 0.1	-210	
	S20061-15	1008	194.6 ± 2.0	-4.7 ± 0.1	-210	
	S20196-01	1806	373.3 ± 2.0	-9.3 ± 0.1	-210	
	S20196-03	1806	276.8 ± 2.0	-6.9 ± 0.1	-210	
	S20196-10	1806	178.3 ± 2.0	-4.0 ± 0.1	-211	
	IBS SiO ₂	S21056-02	1000	238.5 ± 2.0	-13.1 ± 0.1	-571
		S21056-07	1000	137.5 ± 2.0	-7.9 ± 0.1	-577
S22073-01		2032	246.3 ± 2.0	-13.7 ± 0.1	-576	
S22073-03		2032	136.4 ± 2.0	-7.7 ± 0.1	-580	
Thermal SiO ₂	INL-A31	1500	256.7 ± 2.0	-11.3 ± 0.1	-319	
	INL-C05	1500	340.5 ± 2.0	-14.2 ± 0.1	-320	
	INL-A21	1500	506.7 ± 2.0	-20.9 ± 0.1	-323	

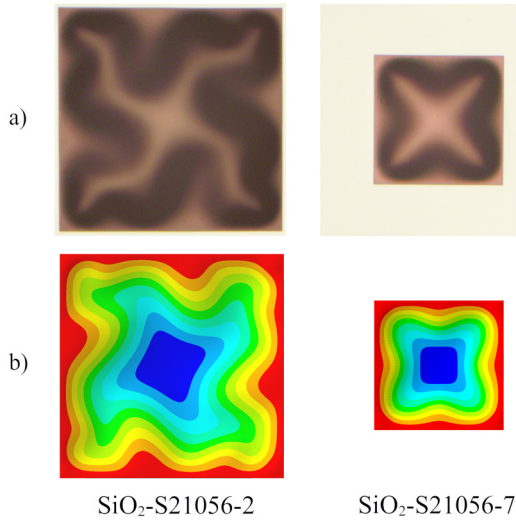


FIG. 2. (a) Photos (top view) and (b) simulated profiles (qualitative appearance) of two IBS SiO₂ membranes.

buckling analysis was performed by defining a compressive bi-axial stress in the material.

In all simulations, the studied film was assumed to be homogeneous and isotropic, with no stress gradient along the film thickness. The values of Young's modulus and Poisson's ratio of the membranes were, respectively, set to 121 GPa and 0.29 for tantalum samples and to 78 GPa and 0.14 for silica samples, as measured on IBS thin films grown under identical conditions;⁹ for thermally grown silica, the values of bulk fused silica were used: 72.8 GPa and

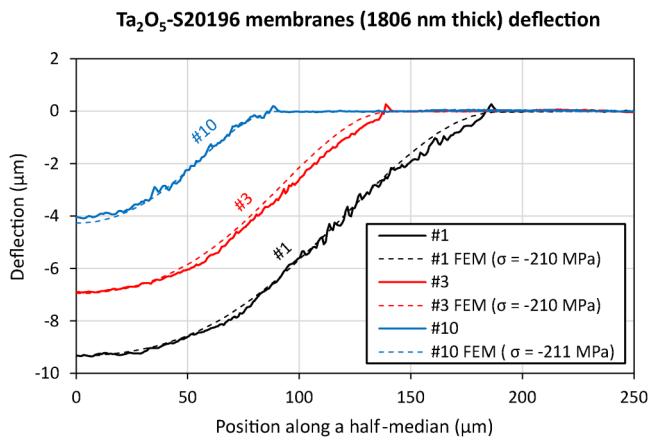


FIG. 3. Measured and simulated deflections for 1806 nm thick IBS Ta₂O₅ membranes (S20196 serie). Membrane characteristics are given in Table I. Solid/dashed lines: measurements/simulations (stress values are given in parenthesis; Young's modulus and Poisson's ratio values of 121 GPa and 0.29, respectively, were used).

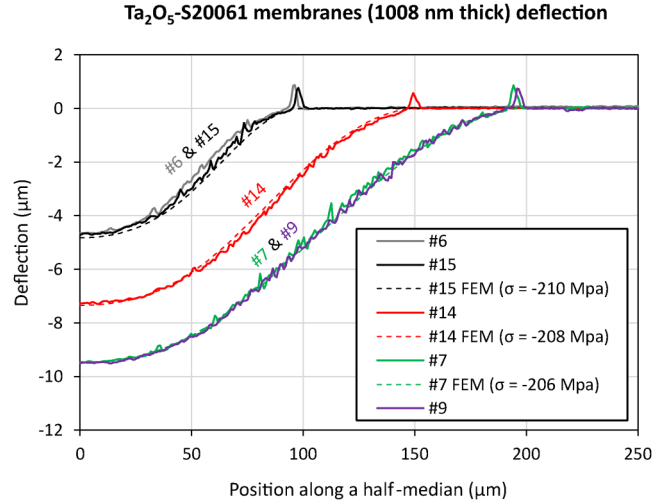


FIG. 4. Measured and simulated deflections for 1008 nm thick IBS Ta₂O₅ membranes (S20061 serie). Membrane characteristics are given in Table I. Solid/dashed lines: measurements/simulations (stress values are given in parenthesis; Young's modulus and Poisson's ratio values of 121 GPa and 0.29, respectively, were used).

0.165, respectively. The dependency of estimated stress values on these two parameters will be discussed in Sec. III.

III. RESULTS AND DISCUSSION

As an example, photos of two IBS SiO₂ membranes and the corresponding simulated profiles are shown in Figs. 2(a) and 2(b),

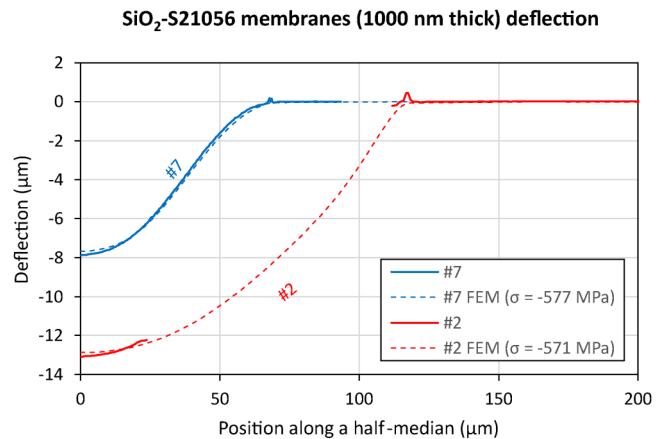


FIG. 5. Measured and simulated deflections for 1000 nm thick IBS SiO₂ membranes (S21056 serie). Membrane characteristics are given in Table I. Solid/dashed lines: measurements/simulations (stress values are given in parenthesis; Young's modulus and Poisson's ratio values of 78 GPa and 0.14, respectively, were used).

22 February 2024 08:39:37

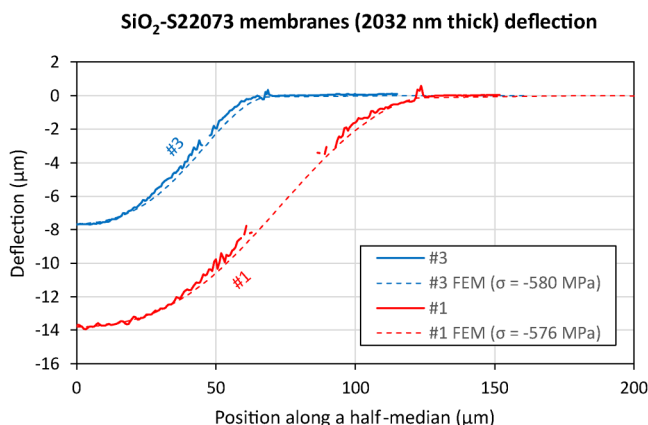


FIG. 6. Measured and simulated deflections for 2032 nm thick IBS SiO₂ membranes (S22073 serie). Membrane characteristics are given in Table I. Solid/dashed lines: measurements/simulations (stress values are given in parenthesis; Young's modulus and Poisson's ratio values of 78 GPa and 0.14, respectively, were used).

respectively. Observed and simulated deflection profiles, as probed along a half median, are compared in Figs. 3 and 4 for IBS Ta₂O₅ membranes and in Figs. 5 and 6 for IBS SiO₂ membranes. Results for membranes of thermal SiO₂ are presented in Fig. 7. Note that for some strongly distorted samples, some experimental data points are missing due to the maximum detectable slope limit set by the objective of the profilometer.

The stress values used in simulations are reported in the right column of Table I. The stress state of IBS Ta₂O₅ membranes is about -209 MPa, whereas the IBS SiO₂ membranes are in a higher

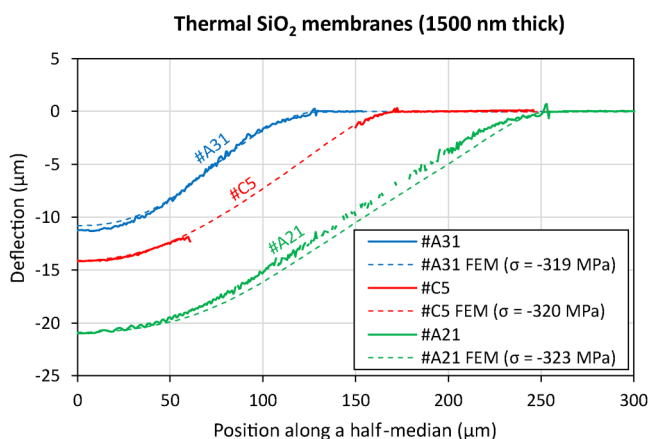


FIG. 7. Measured and simulated deflections for 1500 nm thick thermal SiO₂ membranes. Membrane characteristics are given in Table I. Solid/dashed lines: measurements/simulations (stress values are given in parenthesis, Young's modulus and Poisson's ratio values of 72.8 GPa and 0.165, respectively, were used).

compressive stress state of about -576 MPa. Such values seem to be independent of the sample thickness as shown by comparing S20061 and S20196 Ta₂O₅ samples and S21056 and S22073 SiO₂ samples with close dimensions, as well as from moderate changes of Young's modulus and Poisson's ratio values used in simulations. For the 2032 nm thick IBS SiO₂ membranes, for example, additional simulations were performed with a 7% lower Young's modulus and a 15% higher Poisson's ratio (fused silica elastic parameters), yielding a change of the estimated stress level of only about 1% (-572 and -573 MPa for samples SiO₂-S22073-1 and -3, respectively). This is analogous to the case of a drumhead, whose vibration frequency depends mainly on its tension and not on its rigidity.

The average stress in thermal SiO₂ grown at 1130°C was found equal to -321 MPa, in good agreement with the literature.^{31,32} In this case, the residual stress is mainly due to the mismatch of thermal expansion coefficients of the thermally grown SiO₂ thin film and of the silicon substrate.

Assuming that the thin films' thickness and elastic constants are well known, the relative error on our stress evaluation method can be estimated to be less than 5% due to the uncertainties on the measurements of size and deflection of the membranes. This relative error is comparable, if not slightly better, than that which would be obtained by the substrate curvature method that uses Stoney's equation.

IV. CONCLUSIONS

We developed an alternative method for the determination of compressive stresses in thin films based on measurements and finite-element simulations of buckled self-supporting membranes.

We found that the average stress of IBS Ta₂O₅ thin films is -209 MPa, and that IBS SiO₂ thin films feature a higher average stress of -576 MPa. For comparison, the average stress in thermal SiO₂ grown at 1130°C is found equal to -321 MPa, in good agreement with the literature.

The study of the deflection of buckled membranes appears to be a suitable alternative to the curvature method for the determination of large compressive stresses in thin films. As a large number of samples can be produced out of a single coated substrate, high reliability and repeatability of the results can be obtained. In addition, these very same membranes could be used for many other characterizations: micro-Raman spectroscopy, x-ray diffraction, ion-beam analyses (Rutherford back-scattering and elastic-recoil detection), etc. It may also open up the possibility of probing for stress uniformity across the surface of a substrate or stress changes with composition if there is a composition gradient.

ACKNOWLEDGMENTS

The authors gratefully acknowledge the support of the French Agence Nationale de la Recherche (ANR) through Grant No. ANR-18-CE08-0023 (project ViSIONs) and of the national program Investments for the Future through Grant No. ANR-11-LABX-022-01 (managed by ANR). The membranes were processed at the Plateforme technologique Nanolyon of the Institut des Nanotechnologies de Lyon (INL). The authors thank J. Degouttes for his technical support on this project, and C. Gaillard for access

22 February 2024 08:39:37

to the chemistry laboratory at the *Institut de Physique des deux Infinis de Lyon* (IP2I).

AUTHOR DECLARATIONS

Conflict of Interest

The authors have no conflicts to disclose.

Author Contributions

C. Malhaire: Conceptualization (lead); Data curation (equal); Methodology (lead); Validation (lead); Writing – original draft (lead); Writing – review & editing (equal). **M. Granata:** Data curation (equal); Methodology (supporting); Validation (equal); Writing – original draft (equal); Writing – review & editing (equal). **D. Hofman:** Data curation (supporting); Writing – review & editing (supporting). **A. Amato:** Writing – review & editing (supporting). **V. Martinez:** Writing – review & editing (supporting). **G. Cagnoli:** Funding acquisition (lead); Project administration (lead); Writing – review & editing (supporting). **A. Lemaître:** Validation (supporting); Writing – review & editing (equal). **N. Shcheblanov:** Writing – review & editing (supporting).

DATA AVAILABILITY

The data that support the findings of this study are available within the article.

REFERENCES

- ¹J. Aasi and The LIGO Scientific Collaboration, *Classical Quant. Grav.* **32**, 074001 (2015).
- ²F. Acernese and The Virgo Collaboration, *Classical Quant. Grav.* **32**, 024001 (2014).
- ³Y. Aso, Y. Michimura, K. Somiya, M. Ando, O. Miyakawa, T. Sekiguchi, D. Tatsumi, and H. Yamamoto (The KAGRA Collaboration), *Phys. Rev. D* **88**, 043007 (2013).
- ⁴A. E. Villar *et al.*, *Phys. Rev. D* **81**, 122001 (2010).
- ⁵See <http://lma.in2p3.fr> for the Laboratoire des Matériaux Avancés CNRS/IN2P3 website.
- ⁶L. Pinard *et al.*, *Appl. Opt.* **56**, C11 (2017).
- ⁷J. Degallaix *et al.*, *J. Opt. Soc. Am. A* **36**, C85 (2019).
- ⁸A. Amato *et al.*, *J. Phys.: Mater.* **2**, 035004 (2019).
- ⁹M. Granata *et al.*, *Classical Quant. Grav.* **37**, 095004 (2020).
- ¹⁰P. R. Saulson, *Fundamentals of Interferometric Gravitational Wave Detectors*, 2nd ed. (World Scientific, Singapore, 2017), see <https://www.worldscientific.com/doi/pdf/10.1142/10116>.
- ¹¹M. Granata *et al.*, *Appl. Opt.* **59**, A229 (2020).
- ¹²G. Vajente *et al.*, *Phys. Rev. Lett.* **127**, 071101 (2021).
- ¹³S. Hild *et al.*, *Classical Quant. Grav.* **28**, 094013 (2011).
- ¹⁴ET Steering Committee Editorial Team, “Design Report Update 2020 for the Einstein telescope,” ET technical note ET-0007B-20 (2020), <https://apps.et-gw.eu/tds/ql/?c=15418>.
- ¹⁵E. D. Hall, “Cosmic explorer: a next-generation ground-based gravitational-wave observatory,” *Galaxies* **10**, 90 (2022).
- ¹⁶J. M. Ngaruiya, S. Venkataraj, R. Drese, O. Kappertz, T. P. Leervad Pedersen, and M. Wuttig, *Phys. Status Solidi A* **198**, 99 (2003).
- ¹⁷W. Cheng, S. Chi, and A. Chu, *Thin Solid Films* **347**, 233 (1999).
- ¹⁸M. S. Farhan, E. Zalnezhad, and A. Bushroa, *Mater. Res. Bull.* **48**, 4206 (2013).
- ¹⁹A. Davenport, E. Randel, and C. S. Menoni, *Appl. Opt.* **59**, 1871 (2020).
- ²⁰R. P. Netterfield *et al.*, *Proceedings of the Advances in Thin-Film Coatings for Optical Applications II*, San Diego, CA, 1-2 August 2005, edited by M. L. Fulton and J. D. T. Kruschwitz (SPIE, Bellingham, WA, 2005), Vol. 5870, pp. 144–152.
- ²¹M. Granata *et al.*, *Phys. Rev. D* **93**, 012007 (2016).
- ²²M. Abernathy *et al.*, *Class. Quant. Grav.* **38**, 195021 (2021); [arXiv:2103.14140](https://arxiv.org/abs/2103.14140) [physics.ins-det].
- ²³L. Émile *et al.*, *J. Vac. Sci. Technol. A* **39**, 043416 (2021).
- ²⁴L. Émile, “Synthèse de couches optiques par co-dépôt pour les miroirs de LIGO,” Master’s thesis (Université de Montréal, Faculté des arts et des sciences, Département de physique, 2021).
- ²⁵M. R. Ardigo, M. Ahmed, and A. Besnard, *Residual Stresses IX - Advanced Materials Research, proceedings of the 9th European Conference on Residual Stresses, ECRS-9*, July 7-10, 2014, Troyes, France, edited by M. François, G. Montay, B. Panicaud, D. Reira, and E. Rouhaud (Trans Tech Publications Ltd., Stafa-Zurich, Switzerland, 2014), Vol. 996, pp. 361–366.
- ²⁶C. Malhaire, *Rev. Sci. Instrum.* **83**, 055008 (2012).
- ²⁷P. Martins, C. Malhaire, S. Brida, and D. Barbier, *Microsyst. Technol. Micro Nanosyst. Inform. Storage Process. Syst.* **15**, 1343 (2009).
- ²⁸P. Martins, P. Delobelle, C. Malhaire, S. Brida, and D. Barbier, *Eur. Phys. J.-Appl. Phys.* **45**, 10501 (2009).
- ²⁹V. Ziebart, O. Paul, and H. Baltes, *J. Microelectromech. Syst.* **8**, 423 (1999).
- ³⁰J. I. Cisneros, *Appl. Opt.* **37**, 5262 (1998).
- ³¹R. J. Jaccodine and W. A. Schlegel, *J. Appl. Phys.* **37**, 2429 (1966).
- ³²C. Malhaire, M. Le Berre, D. Febvre, D. Barbier, and P. Pinard, *Sens. Actuators A: Phys.* **74**, 174 (1999).

22 February 2024 08:39:37